Encoding of Olfactory Information with Oscillating Neural Assemblies

Gilles Laurent* and Hananel Davidowitz

In the brain, fast oscillations of local field potentials, which are thought to arise from the coherent and rhythmic activity of large numbers of neurons, were observed first in the olfactory system and have since been described in many neocortical areas. The importance of these oscillations in information coding, however, is controversial. Here, local field potential and intracellular recordings were obtained from the antennal lobe and mushroom body of the locust *Schistocerca americana*. Different odors evoked coherent oscillations in different, but usually overlapping, ensembles of neurons. The phase of firing of individual neurons relative to the population was not dependent on the odor. The components of a coherently oscillating ensemble of neurons changed over the duration of a single exposure to an odor. It is thus proposed that odors are encoded by specific but dynamic assemblies of coherently oscillating neurons. Such distributed and temporal representation of complex sensory signals may facilitate combinatorial coding and associative learning in these, and possibly other, sensory networks.

The widespread occurrence of local field potential oscillations in olfactory systems (*1–3*) suggests that synchronized neuronal activity (*4, 5*) may play a fundamental role in the processing of odor-evoked signals. We examined this hypothesis by focusing on the olfactory nervous system of insects. Insects rely on olfaction for detection and recognition of mates and kin, for food localization, and for communication (*6*). Remarkably, the architecture of their olfactory nervous system shows many fundamental similarities to that of vertebrates, which suggests convergent evolution of circuit designs: A large number (about 50,000) of receptor neurons in the antenna converge onto a glomerular neuropil (*7*), the antennal lobe, which is analogous to the vertebrate olfactory bulb. Here, dendrodendritic interactions occur between excitatory projection neurons (PNs) and inhibitory local neurons (LNs) (*8*) (Fig. 1A). The PNs project to the mushroom body, which is a large distributed network of neurons associated with memory functions (*9*), as is the piriform cortex, the corresponding structure in the vertebrate brain (*10*).

We examined odor processing in both mushroom bodies and antennal lobes of the locust *Schistocerca americana*, using electrophysiological techniques in vivo (*11*). Upon presentation of airborne odorants, oscillations of local field potentials were evoked in the mushroom bodies for a duration similar to that of the odor puff (n = 73 animals) (*12*). The oscillations were characterized by a narrow spectral peak (19.0 ± 3.6 Hz, n = 16) that was independent of the odor. No oscillation occurred when air alone was puffed or when the antennae were removed. The oscillations, examined with cross-correlation techniques (*13*), were broadly distributed and spatially coherent, as simultaneous recordings from distant sites were highly correlated with no phase lag, which indicates the absence of traveling waves (Fig. 1, B through E). The cross-correlation patterns evoked by several odors in the same animal were generally not distinguishable (such as those evoked by cherry and isoamylacetate in Fig. 1, D through E). However, subtle odor-specific differences were occasionally observed in the temporal features of the cross-correlation: The apple odor evoked oscillations of steadily decreasing frequency, whereas cherry or isoamylacetate did not (Fig. 1, C through E).

To determine whether the field potential oscillations observed in the mushroom bodies were generated locally or were driven by os-

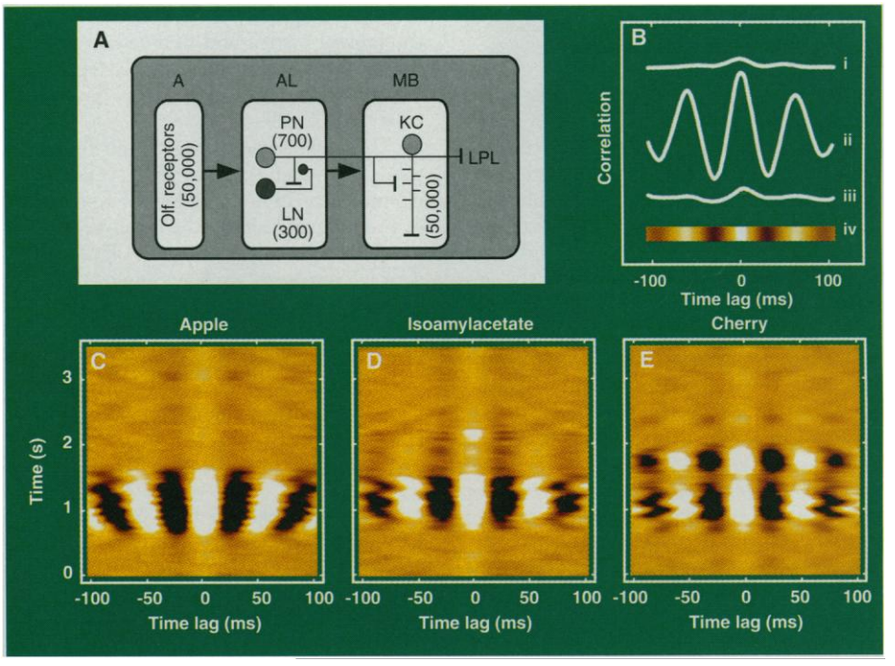

Fig. 1. (**A**) Schematic representation of the olfactory circuits. A, antenna; AL, antennal lobe; KC, Kenyon cell; LN, local neuron; LPL, lateral protocerebral lobe; MB, mushroom body; PN, projection neuron; approximate number of neurons is in brackets (*7, 8*). (**B**) Cross-correlation function between two simultaneously recorded local field potentials in the mushroom body (*11, 13*) for three time windows after (i), during (ii), and before (iii) the response to an odor pulse. The time lag against which the correlation function is plotted represents the amount by which one field potential is progressively shifted relative to the other for the computation of the cross-correlation. A peak at 0 ms, for example, indicates a positive correlation between the two signals and the absence of a phase difference between them. Peaks at ± 50 ms (ii) indicate that, if the amplitude of the field potential at one site is high at time t, the amplitude of the field potential at the second site is likely to be high also at t − 50 ms and t + 50 ms. The cross-correlation was calculated piecewise (*11, 13*) over 3.4 s. For each window, the amplitude of the correlation function (i through iii) at each instant was assigned a color (white, high; orange, intermediate; black, low) to form an intensity-coded bar (iv). The color bar in (iv) represents the correlation function in (ii). These intensity-coded bars were then stacked [(C) through (E)] to visualize the changes in the cross-correlation around the time of an odor delivery. (**C** through **E**) Cross-correlations calculated between the two local field potentials for three different odors (~300 μm between electrodes). These cross-correlations were calculated for single odor presentations and in the same animal. The odors were applied in 1-s-long pulses (offset at 0.5 s). (Time runs along the y axis, and the time lag of the correlation function runs along the x axis.) The double burst evoked by cherry here was singular and was probably caused by local air turbulence.

cillatory input from the antennal lobes, we examined the relation between oscillations in the mushroom bodies and the activity of single PNs and LNs in the antennal lobes (Fig. 2). Intracellular recordings from 109 PNs revealed odor-evoked membrane potential oscillations that were correlated with the field potentials (Fig. 2A, panel i). These oscillations consisted of alternating excitatory and inhibitory postsynaptic potentials (EPSPs and (EPSPs) that maintained a fixed phase relative to the field potential oscillations in the ipsilateral mushroom body (Fig. 2). PN spikes occurred in the ascending phase of the field potential (phase = $-70° \pm 52$, mean ± SD, $n = 210$ cycles, where 0° is defined as the peak of the field potential) (Fig. 2B, panel i). The onset of the IPSPs coincided with the rest of the field potential, thereby inhibiting spiking during the descending phase of the field potential (phase = $16° \pm 26$, $n = 210$ cycles) (Fig. 2B, panel ii). The other antennal lobe neurons (LNs) are axonless, GABA-ergic, and known from electron microscope studies to contact PNs directly (*14*).

We recorded intracellularly the activity of 68 LNs (from their dendrites) during olfactory processing and established that they too oscillate in phase with the field potential in the mushroom bodies (Fig. 2A, panel ii). LNs produced no conventional overshooting action potentials but produced graded tetrodotoxin-resistant active potentials. These potentials (or the peak of the underlying depolarizing waves) coincided with the peak of the field potentials (phase = $23° \pm 27$, $n = 203$ cycles) (Fig. 2B, panel iii), which indicates that they probably underlie the regular IPSPs in PNs (*15*). The phase of PN and LN activity was odor-independent [for example, an LN phase was $19° \pm 12$ for citrus and $23° \pm 17$ for apple, which are not significantly different from one another ($P < 0.001$, paired t test)]. This result indicates that odor quality is not encoded in the phase of firing of individual neurons. The odor-evoked membrane potential oscillations of PNs and LNs remained after surgical ablation of the mushroom bodies (seven animals), which shows that the oscillations are endogenous to the antennal lobes and suggests that the LFP oscillations in the mushroom bodies are at least partly a consequence of oscillatory drive from the antennal lobe PNs.

Because antennal lobe neurons oscillate in response to odorants, we asked whether odor qualities are represented neurally by specific assemblies of coherently firing neurons. Such distributed representation would thus allow combinatorial coding, in which each odor-encoding set of neurons would be defined by its synchronized firing. The first requirement for such a coding scheme is that not all antennal lobe neurons oscillate in response to all odorants. In 177 (LN and PN) neurons studied, membrane potential oscillations and rhythmic firing occurred only in response to some (and sometimes none) of the odors tested (*16*). One PN, for example, was rhythmically active when cherry (Fig. 3A, panel i) or pine odors were presented. When an apple or floral scent was presented, this PN was inhibited and no rhythmic modulation of membrane potential occurred (Fig. 3A, panels ii and iii). In each odor presentation, however, the field potential showed oscillations, which indicates that other antennal lobe neurons were rhythmically active at that time. When apple and cherry odors were presented concurrently, this PN remained inhibited and several IPSPs but no EPSPs were observed

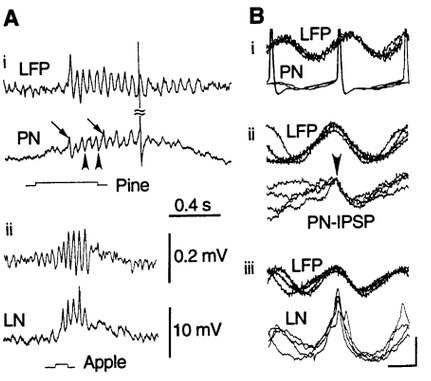

Fig. 2. PN somata and LN dendrites were impaled in vivo in the antennal lobe while local field potentials (LFP) were recorded from the ipsilateral mushroom body. (**A**) (i) Alternating EPSPs (arrows) and IPSPs (arrowheads) evoked in a PN by a puff of airborne pine odor are phase-locked to the field potential. The PN was held hyperpolarized to reveal the underlying synaptic drive (*12*). (ii) Odor-evoked oscillatory activity in a LN, phase-locked to the field potential. (**B**) Superimposed traces triggered from (i) PN action potential at center, (ii) onset of PN-IPSP (arrowhead), (iii) peak of fluctuations in LN potential during odor-evoked oscillations. Calibration: horizontal, 20 ms; vertical, 0.1 mV (LFP), 20 mV (PN) (i), 1 mV (PN) (ii), and 4 mV (LN) (iii).

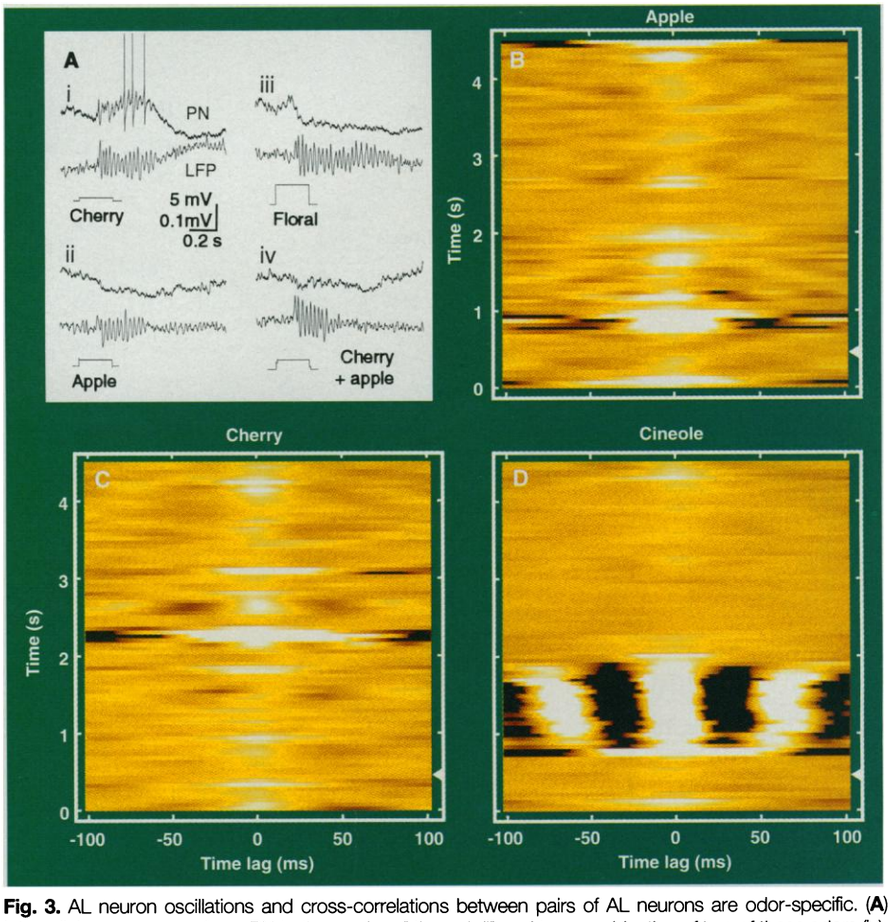

Fig. 3. AL neuron oscillations and cross-correlations between pairs of AL neurons are odor-specific. (**A**) Intracellular responses of one PN to three odors (i through iii) and to a combination of two of these odors (iv). (**B** through **D**) Cross-correlations calculated between the membrane potentials of a pair of LNs recorded simultaneously during single presentations of apple (B), cherry (C), and cineole (D). The representation of the cross-correlograms is as in Fig. 1, C through E. Arrowheads indicate ends of 1-s-long odor puffs.

Biology Division, California Institute of Technology, Pasadena, CA 91125, USA.

*To whom correspondence should be addressed.

(Fig. 3A, panel iv). The absence of the periodic EPSPs caused by cherry alone (Fig. 3A, panel i) suggests that the neurons from which they originated were inactivated or desynchronized by the apple scent (Fig. 3A, panel iv). This indicates that the ensembles of neurons that code for different odors overlap.

The second requirement for this coding scheme is that the firing of the neurons forming an oscillatory assembly be coherent on a cycle-by-cycle basis and not simply on average, as calculated over many successive odor presentations. We therefore recorded intracellularly from 56 pairs of antennal lobe neurons and examined the cross-correlation of their activities during single-odor presentations. In the pair of LNs shown in Fig. 3, B through D, for example, cineole clearly led to a correlated oscillatory response, but apple or cherry did not. This demonstrates that oscillations of this pair of neurons are both synchronized and odor-specific. The response patterns of 38 PNs and the coherently oscillating ensembles they form upon odor presentation are summarized in Table 1. Different odors evoke coherent oscillatory activity of specific and overlapping ensembles of neurons.

The response of a single neuron was often not continuous during presentation of a single odor. Of the 109 PNs studied, 103 fired during only a portion of the odor-evoked field potential oscillations. Thus, the response of a neuron to an odor often consisted of successive segments of excitation and inhibition (*17*) that were specific to the odor-neuron combination (Table 1). The PN in Fig. 4A, for example, although excited by at least three distinct odors, responded differently to each one of them. Its response to apple was monophasic, while those to mint or citrus were multiphasic. A pronounced inhibition terminated the activity evoked by citrus and temporarily interrupted that evoked by mint. The mono- and multiphasic response patterns of 38 other PNs to five odorants (at identical concentrations) are shown in Table 1. Although individual neurons were temporarily inhibited, the field potentials were not interrupted, because other neurons responded in an antagonistic fashion. A pair of simultaneously recorded PNs, for example, responded with opposed temporal patterns to isoamylacetate or cineole (Fig. 4B). Finally, we observed that an antennal lobe neuron that is transiently activated by an odor is not necessarily synchronized to the oscillating population during that time (n = 25 neurons). Spikes evoked by mint in the neuron in Fig. 4A, for example, were synchronized with the population only during the second excitatory segment of its response (Fig. 4C, right panel). Other neurons were synchronized during the early portion of the response, however, as demonstrated by the existence of field potential oscillations (Fig. 4C, left panel). A PN can therefore fire action potentials in response to an odor without showing rhythmic activity that is synchronized with the ensemble that causes the 20-Hz field potential oscillations. Such absence of synchronization is often transient.

Table 1. Response properties of 38 PNs (rows) to five odors (i.a.a., isoamylacetate) (0, no response; E, excitation; dE, delayed E (about 1 s of delay); I, inhibition; dash, not tested). The shaded boxes indicate neurons that oscillated in phase with the local field potential during the first third of the duration of the local field potential oscillation. Odor pulses were 1 s long.

Apple	Cherry	Cineole	Cinnamon	I.A.A.
0	0	IIE	0	I
EIE	0	IE	0	E
0	EIE	I	0	IE
0	I	EIE	0	EIE
IE	IE	IE	0	I
E	E	II	0	EIE
I	E	IE	0	I
I	0	I	I	0
0	0	EI	E	0
I	E	EIE	I	0
I	I	0	0	-
IE	0	E	0	-
EI	IE	I	E	-
IE	I	I	0	-
EIE	IE	I	E	-
I	0	I	0	-
0	EI	E	0	-
I	I	E	I	-
0	0	0	I	-
0	0	E	E	-
0	IE	I	I	-
0	I	E	I	-
0	E	I	I	-
I	I	0	0	-
E	EIE	I	EI	-
I	IE	0	0	-
I	IE	I	dE	-
E	I	0	E	-
EI	I	I	0	-
0	EIE	0	-	I
I	E	IE	-	IE
E	0	E	-	I
I	E	0	-	0
EE	0	EI	-	0
0	0	I	-	EI
I	EEE	I	-	I
0	I	0	-	0
0	E	I	-	I

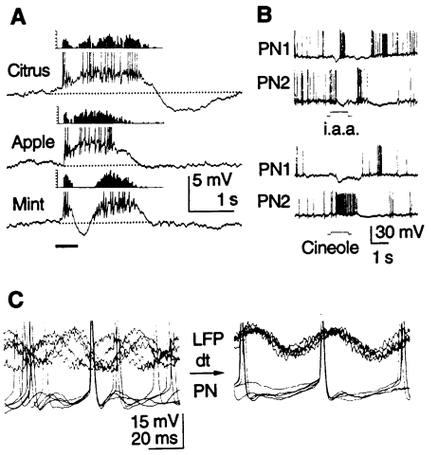

Fig. 4. Individual AL neurons often participate in coherent oscillations during a fraction only of the duration of the field potential oscillations. (**A**) Response of one PN to three odors. Odor delivery is indicated by the horizontal bar. Insets: cumulative spike frequency histograms constructed from 20 consecutive responses to each odor, showing consistency of patterns (two spikes per tick mark). Spikes are clipped. (**B**) Intracellular recordings from a pair of PNs show antagonism and activity patterns that differ for these two odors (i.a.a., isoamylacetate). (**C**) Superimposed traces triggered from the spikes in the two successive bursts evoked by mint in the PN in (A) [bottom trace in (A)]. Left panel: traces from short initial burst; dt, time interval during which the interneuron is silent; right panel: traces from long final burst. Local field potential (LFP) was recorded in the mushroom body (calibration: 200 μV).

In summary, all odors tested evoke synchronous 20-Hz field potential oscillations in the mushroom bodies that are driven by the coherent oscillatory activity of antennal lobe PNs and LNs. Each odor tested produces synchronized oscillations in a specific ensemble of PNs (and LNs) during part of the response. By exclusion, this defines another set of antennal lobe neurons that are not synchronized, because they are either inhibited, unaffected, or excited but not phase-locked to the field potential. Each odor can thus be defined by an assembly of coherently firing antennal lobe neurons. Because antennal lobe neurons are generally activated by several odors, the assemblies that encode different odors can overlap (*18*). An antennal lobe neuron often participates in the synchronized output only during a fraction of the period over which collective oscillations occur. The window during which a neuron is synchronized with others is the same for successive presentations of a given odor at one concentration. We therefore propose that odor quality is encoded not only by an assembly of synchronously oscillating neurons but by a particular succession of different, but overlapping, oscillating assemblies. Such progressive transformation of the oscillating population might possibly be used to encode spatiotemporal gradients in the stimulus, rather than odor identity (*19*). Because many PNs converge on each mushroom body interneuron (*20*), associative memory processes in the mushroom bodies (*9*) may depend on the odor-specific temporal overlap of firing of converging PNs. We showed that this overlap is determined by at least two processes: a fast, recurrent one (the 20-Hz oscillations) and a slow one (the windows during which a given PN participates in the oscillations).

Because these olfactory networks show many topological similarities to those of the vertebrate olfactory system, we propose that the olfactory bulb and perhaps other vertebrate (*2*, *4*) and invertebrate (*3*) brain circuits may use similar combinatorial computational principles. It is tempting to speculate that oscillations in the visual cortex of mammals (*4*), for example, serve a purpose in assembly coding that is similar to that described here.

REFERENCES AND NOTES

1. Brain local field potentials, which are recorded extracellularly, are caused by the superposition of extracellular currents generated by the activation of transmembrane voltage-gated and (mainly) synaptic conductances in nearby neurons.
2. E. D. Adrian, *J. Physiol. (London)* **100**, 459 (1942); W. J. Freeman, *J. Neurophysiol.* **35**, 762 (1972); L. B. Haberly, *Chem. Senses* **10**, 219 (1985).
3. A. Gelperin and D. W. Tank, *Nature* **435**, 437 (1990); K. R. Delaney *et al.*, *Proc. Natl. Acad. Sci. U.S.A.* **91**, 669 (1994).
4. J. J. Bouyer *et al.*, *Neuroscience* **22**, 863 (1987); R. Eckhorn *et al.*, *Biol. Cybern.* **60**, 121 (1988); C. M. Gray and W. Singer, *Proc. Natl. Acad. Sci. U.S.A.* **86**, 1698 (1989); V. N. Murthy and E. E. Fetz, *ibid.* **89**, 5670 (1992).
5. F. Crick and C. Koch, *Cold Spring Harbor Symp. Quant. Biol.* **55**, 953 (1990); Z. Li and J. J. Hopfield, *Biol. Cybern.* **61**, 379 (1989); W. Singer, *Annu. Rev. Physiol.* **55**, 349 (1992); H. Sompolinsky, D. Golomb, D. Kleinfeld, *Proc. Natl. Acad. Sci. U.S.A.* **87**, 7200 (1990); C. Von der Malsburg and W. Schneider, *Biol. Cybern.* **54**, 29 (1986).
6. F. G. Barth, *Insect and Flowers: The Biology of a Partnership* (Princeton Univ. Press, Princeton, NJ, ed. 1, 1985); E. O. Wilson, *The Insect Societies* (Harvard Univ. Press, Cambridge, MA, ed. 5, 1979).
7. C. Masson and H. Mustaparta, *Physiol. Rev.* **70**, 199 (1990). The prevailing view is that the antennal receptor neurons synapse directly at least onto the local neurons (*8*).
8. J. Boeckh and K. D. Ernst, *J. Comp. Physiol.* **161A**, 549 (1987); U. Homberg, T. A. Christensen, J. G. Hildebrand, *Annu. Rev. Entomol.* **34**, 477 (1989); B. Waldrop, T. A. Christensen, J. G. Hildebrand, *J. Comp. Physiol.* **161A**, 23 (1987).
9. R. L. Davis, *Neuron* **11**, 1 (1993); R. Menzel, in *Memory Traces in Honeybees. Neurobiology and Behavior of Honeybees*, R. Menzel and A. Mercer, Eds. (Springer-Verlag, Berlin, Germany, ed. 1, 1987), pp. 310–325.
10. L. B. Haberly and J. M. Bower, *Trends Neurosci.* **12**, 258 (1989); M. E. Hasselmo *et al.*, *Cold Spring Harbor Symp. Quant. Biol.* **55**, 599 (1990).
11. Experiments were carried out in vivo with adult locusts of both sexes. The brain was supported by a wax-coated platform inserted between the connectives and was superfused with physiological saline [140 mM NaCl, 5 mM KCl, 5 mM $CaCl_2$, 4 mM $NaHCO_3$, 1 mM $MgCl_2$, 6.3 mM Hepes (pH 7.1)] at room temperature. Local field potentials were recorded with patch pipettes filled with saline (~1 megohm) that were connected to a dc amplifier and low-pass filtered on-line with an eight-pole digital Butterworth filter (Model 9002, Frequency Devices, Haverhill, MA) or off-line with a Savitsky-Golay algorithm (*13*). Local field potentials were recorded in the mushroom body from two sites that are usually separated by 200 to 400 μm. Intracellular recordings from antennal lobe neurons were made with potassium acetate–filled microelectrodes (80 to 120 megohm) and an Axoclamp 2A amplifier (Axon Instruments, Foster City, CA). Airborne odors were delivered to the antenna with five Teflon-coated steel tubes in gentle pressure pulses controlled by electrical and pneumatic valves.
12. A variable delay (up to several hundred milliseconds) was usually observed between the onset of the current pulse triggering the odor delivery and the onset of the physiological response in the antennal lobe or mushroom body. This delay is explained by the lag time separating the openings of the electrical and pneumatic valves and by the distance separating the odor delivery tubes from the antenna (up to 5 cm), which caused long transport times. Such long distances were chosen to minimize stimulation of antennal mechanoreceptors.
13. Field potential and intracellular data were digitized at 5 kHz with a TL1-DMA board (Axon Instruments). To produce the cross-correlograms, the electrophysiological traces typically were broken up into about 240 (or 120) windows of 1024 points. Each window overlapped the next one by 896 (or 768) points. The data were digitally filtered with a fourth-degree Savitsky-Golay smoothing algorithm (using 257 or 513 points) (W. H. Press *et al.*, *Numerical Recipes in C*, Cambridge Univ. Press, Cambridge, ed. 2, 1992). The filtering and cross-correlation algorithms were written in MATHEMATICA and run on NeXTstation and Silicon Graphics Indigo platforms.
14. S. G. Hoskins *et al.*, *Cell Tissue Res.* **244**, 243 (1986); D. Malun, *Histochemistry* **96**, 197 (1991).
15. A direct physiological demonstration of an inhibitory synapse was obtained for one LN-PN pair.
16. The number of odors routinely tested with each neuron varied from 4 to 15.
17. Slow modulation of firing has been observed in female-pheromone-sensitive interneurons in cockroaches [M. Burrows, J. Boeckh, J. Esslen, *J. Comp. Physiol.* **145A**, 447 (1982)], in *Manduca sexta* [R. Kanzaki *et al.*, *ibid.* **165A**, 427 (1989)], and in mammalian [M. Meredith, *J. Neurophysiol.* **56**, 572 (1986)] and amphibian [K. A. Hamilton and J. S. Kauer, *ibid.* **59**, 1736 (1988)] olfactory bulbs.
18. See J. S. Kauer and A. R. Cinelli, *Micr. Res. Tech.* **24**, 157 (1993) for suggestions for modular and overlapping representation of odors in the olfactory bulb.
19. See "the concentration tuning" hypothesis [J. S. Kauer, *J. Physiol. (London)* **243**, 695 (1974)].
20. G. Laurent and M. Naraghi, *J. Neurosci.* **14**, 2993 (1994).

21. Funded by McKnight Scholar and NSF-PFF awards (G.L.) and by the Chaim Weizmann Fellowship (H.D.). We are grateful to E. M. Schuman, E. Marder, C. Koch, and S. E. Fraser for their many helpful comments on this manuscript.

13 April 1994; accepted 24 June 1994

Enhanced Aggressive Behavior in Mice Lacking 5-HT_{1B} Receptor

Frédéric Saudou, Djamel Aït Amara, Andrée Dierich, Marianne LeMeur, Sylvie Ramboz,* Louis Segu, Marie-Christine Buhot, René Hen*

The neuromodulator serotonin (5-hydroxytryptamine, 5-HT) has been associated with mood disorders such as depression, anxiety, and impulsive violence. To define the contribution of 5-HT receptor subtypes to behavior, mutant mice lacking the 5-HT_{1B} receptor were generated by homologous recombination. These mice did not exhibit any obvious developmental or behavioral defects. However, the hyperlocomotor effect of the 5-HT_{1A}/$_{1B}$ agonist RU24969 was absent in mutant mice, indicating that this effect is mediated by 5-HT_{1B} receptors. Moreover, when confronted with an intruder, mutant mice attacked the intruder faster and more intensely than did wild-type mice, suggesting the participation of 5-HT_{1B} receptors in aggressive behavior.

Serotonergic drugs are used to treat migraine, depression, and anxiety, and a serotonin deficit has been associated with behaviors such as suicide, impulsive violence, depression, and alcoholism (*1*). The multiple actions of serotonin are mediated by the interaction of this amine with at least 14 receptors (*2*), most of which belong to the GTP-binding protein (G protein)–coupled receptor family.

The 5-HT_{1B} receptor, which is the rodent homolog of the human 5-$HT_{1D\beta}$ receptor, is expressed in a variety of brain regions, including the basal ganglia, central gray, hippocampus, and raphe nuclei (*3*, *4*). Pharmacological studies with weak specific agonists have suggested that activation of 5-HT_{1B} receptors might lead to an increase in anxiety and locomotion and to a decrease in food intake, sexual activity, and aggressive behavior (*5*). The consequences of a blockade of 5-HT_{1B} receptors or of their human counterpart are unknown because there are no specific antagonists for these receptors.

To study the function of the 5-HT_{1B} receptor, we have generated by homologous recombination in embryonic stem (ES) cells homozygous mutant mice lacking both copies of the gene encoding the 5-HT_{1B} receptor (*6*, *7*). Four positive ES cell clones were obtained with both the JA and the JB targeting vectors (Fig. 1 and Table 1). Southern (DNA) blot analyses with Xba I digests and the E2A1 probe or the *neo* probe confirmed that accurate targeting occurred and that no additional integration took place. Cells from the positive clones JA7 and JB13 were microinjected into 3.5-day C57BL/6 mouse blastocysts. The two clones gave rise to highly chimeric mice, which were bred with C57BL/6 females to test for germline transmission of the mutated 5-HT_{1B} receptor gene. The positive chimeras were bred with females from the 129/Sv-ter inbred strain to obtain heterozygotes on the 129/Sv-ter genetic background. Homozygous animals were generated by heterozygote crossings, and the expected 1:2:1 ratio of wild-type (WT), heterozygous, and

F. Saudou, A. Dierich, M. LeMeur, S. Ramboz, R. Hen, Laboratoire de Génétique Moléculaire des Eucaryotes du CNRS, U184 de l'INSERM, Faculté de Médecine, 11 rue Humann, 67085 Strasbourg Cédex, France.
D. Aït Amara, L. Segu, M.-C. Buhot, CNRS, Groupe de Recherche Neurosciences, Equipe Mémoire et Récepteurs Sérotonine, BP71, 13402 Marseille Cédex 20, France.

*Present address: Center for Neurobiology and Behavior, Columbia University, 722 West 168 Street, New York, NY 10032, USA.